EPR Detection of Glutathiyl and Hemoglobin-cysteinyl Radicals during the Interaction of Peroxynitrite with Human Erythrocytes†

Ohara Augusto,*,‡ Silvia Lopes de Menezes,‡ Edlaine Linares,‡ Natália Romero,§ Rafael Radi,|| and Ana Denicola§

Departamento de Bioquímica, Instituto de Química, Universidade de São Paulo, Brazil, and Department of Physical Biochemistry, Facultad de Ciências, and Department of Biochemistry, Facultad de Medicina, Universidade de la Republica, Uruguay

Received May 31, 2002; Revised Manuscript Received September 23, 2002

ABSTRACT: Peroxynitrite, which is formed by the fast reaction between nitric oxide and superoxide anion, has been receiving increasing attention as a mediator of human diseases. An initial controversy about the possibility of free radical production from peroxynitrite in test tubes has been resolved, and presently it is important to establish whether peroxynitrite produces radicals in cells. Here we employed the EPR spin trapping methodology with 5,5-dimethylpyrroline *N*-oxide (DMPO) to study the interaction of peroxynitrite with human erythrocytes. The results confirmed previous findings in demonstrating that oxyhemoglobin is the main target of peroxynitrite in erythrocytes. As we first show here, the produced ferryl-hemoglobin oxidizes its own amino acids and, most probably, amino acids from other hemoglobin monomers to produce hemoglobin-tyrosyl and hemoglobin-cysteinyl radicals. In parallel, ferryl-hemoglobin also oxidizes intracellular glutathione to produce the glutathiyl radical. The EPR spectrum of both DMPO/•cysteinyl-hemoglobin (a^{β}_{H} = 15.4 G) and DMPO/•tyrosyl-hemoglobin (a^{β}_{H} = 8.8 G) radical adducts was characterized. It is proposed that erythrocytes can be efficient peroxynitrite scavengers in vivo through the coupled action of oxyhemoglobin and glutathione. Overall, the results indicate that, through the intermediacy of carbon dioxide and/or hemoproteins, oxidation of glutathione to the glutathiyl radical is likely to be an important consequence of peroxynitrite production in vivo.

The recent understanding of the biochemical reactions of peroxynitrite ($ONOO^- + ONOOH$)[1] has provided support for the view that free radicals may play a role in the biodamaging and bioregulatory roles of the oxidant (*1*, *2* and references therein). Indeed, peroxynitrite is stable at alkaline pHs but upon protonation ($pK_a = 6.6$) decomposes rapidly ($k = 0.17\ s^{-1}$ at 25 °C) to yield ca. 70% nitrate and 30% hydroxyl radical and nitrogen dioxide (eqs 1 and 2), which can oxidize biotargets to the corresponding radicals. However, peroxynitrite oxidations mediated by hydroxyl and nitrogen dioxide radicals are predicted to be important only in biological environments of low pHs because, at neutral pHs, proton-catalyzed peroxynitrite decomposition is too slow to compete with biotargets that can react directly with the oxidant. The most important biological targets are likely to be carbon dioxide, hemoproteins, and thiol-containing compounds because of their biological concentrations and fast bimolecular reactions with peroxynitrite. These reactions greatly reduce the half-life of the oxidant from seconds to milliseconds, and the biotargets are usually oxidized by two-electron mechanisms. One important exception is the direct reaction of peroxynitrite with the biologically ubiquitous carbon dioxide that produces ca. 65% nitrate and 35% carbonate radical anion and nitrogen dioxide (eq 3).

$$ONOO^- + H^+ \rightleftarrows ONOOH \quad (1)$$

$$ONOOH \rightarrow 0.71NO_3^- + 0.71H^+ + 0.29^{\bullet}NO_2 + 0.29^{\bullet}OH \quad (2)$$

$$ONOO^- + CO_2 \rightarrow [ONOOCO_2^-] \rightarrow 0.65NO_3^- + 0.65CO_2 + 0.35^{\bullet}NO_2 + 0.35CO_3^{\bullet -} \quad (3)$$

By competing with other biological targets for the oxidant, carbon dioxide may inhibit their two-electron oxidation, but most of the target that is oxidized will be oxidized by the produced carbonate radical anion and nitrogen dioxide radicals. As a consequence, carbon dioxide may divert biotarget oxidation from two- to one-electron mechanisms particularly at neutral pHs, as clearly demonstrated in the case of peroxynitrite-mediated oxidation of biothiols in vitro (*3*). Since the concentration of the bicarbonate/carbon dioxide pair is high in most biological environments, peroxynitrite-mediated oxidation of biomolecules to radical intermediates is likely to be a recurrent event in vivo.

† This work was supported by grants from the Fundação de Amparo à Pesquisa do Estado de São Paulo (FAPESP), Conselho Nacional de Desenvolvimento Científico e Tecnológico (CNPq), and Financiadora de Estudos e Projetos (FINEP) to O.A., Howard Hughes Medical Institute to R.R., and Comisión Sectorial de Investigación Científica to A.D. S.L.D.M. and N.R. were supported by fellowships from CNPq and PEDECIBA, respectively.

* To whom correspondence should be addressed at the Instituto de Química, Universidade de São Paulo, Cx. P. 26077, 05513-970 São Paulo SP, Brazil. Phone: 55-11-3091-3873. Fax: 55-11-30912186. E-mail: oaugusto@iq.usp.br.

‡ Universidade de São Paulo.

§ Facultad de Ciências, Universidade de la Repulbica.

|| Facultad de Medicina, Universidade de la Republica.

[1] Abbreviations: DMPO, 5,5-dimethylpyrroline *N*-oxide; PBS, isotonic phosphate buffer; peroxynitrite, the sum of peroxynitrite anion ($ONOO^-$, oxoperoxonitrate(1−)) and peroxynitrous acid (ONOOH, hydrogen oxoperoxonitrate) unless specified.

10.1021/bi0262202 CCC: $22.00
Published on Web 11/09/2002

Relevantly, recent EPR spin trapping studies have demonstrated intracellular radical production upon peroxynitrite addition to cells such as erythrocytes (*3*) and macrophages (*4*) even in the absence of added carbon dioxide. The mechanisms of free radical production, however, have not been completely elucidated. Erythrocytes and macrophages are markedly different cell types and are expected to produce radicals by diverse routes upon interaction with peroxynitrite. A first step to elucidate these routes is to characterize the produced radicals. This is not an easy task in cells because they require the use of EPR methodologies that rely on spin traps whose ability to trap different radicals vary substantially (*5*). For instance, although the high oxyhemoglobin concentration in erythrocytes makes it the preferential peroxynitrite target (*6*, *7*), the reported exclusive detection of a hemoglobin-tyrosyl radical in peroxynitrite-treated erythrocytes could be a consequence of the use of a nitroso spin trap (*3*). Accordingly, in the case of peroxynitrite-treated macrophages, production of tyrosyl-protein and glutathiyl radicals was demonstrated with a nitroso and a nitrone (DMPO) spin trap, respectively (*4*). Indeed, nitroso spin traps are not adequate to trap thiyl radicals, whereas nitrone spin traps, DMPO in particular, are (*5*). The detection of the glutathiyl radical in macrophages treated with peroxynitrite (*4*) and the importance of glutathione in maintaining cellular redox balance (*8*) led us to reexamine the interaction of the oxidant with human erythrocytes in the presence of DMPO. The results obtained provide new clues for the understanding of free radical production from peroxynitrite in cells.

EXPERIMENTAL PROCEDURES

Chemicals. All reagents were purchased from Sigma, Merck, or Fisher and were analytical grade or better. Commercial DMPO (Sigma) was vacuum distilled prior to use. Peroxynitrite was synthesized from sodium nitrite (0.6 M) and hydrogen peroxide (0.65 M) in a quenched-flow reactor. To eliminate excess hydrogen peroxide, the peroxynitrite solution was treated with manganese dioxide. Synthesized peroxynitrite contained low levels of contaminating hydrogen peroxide (<1%) and nitrite (10−30%) that were determined as previously described (*9*). The concentration of peroxynitrite stock solutions was determined spectrophotometrically at 302 nm using an extinction coefficient of 1.67 $\times$ 10^3 M^{-1}·cm^{-1} (*9*). Concentrations of CO_2 were calculated from the added HCO_3^- concentrations by using pK_a = 6.4 (*10*). Buffers were pretreated with Chelex-100 to remove contaminant metal ions. All solutions were prepared with distilled water purified with a Millipore Milli-Q system.

Erythrocytes. Fresh heparinized human blood was centrifuged at 3000 rpm for 15 min at 4 °C. The plasma and buffy coat were discarded, and the cells washed with 5 mM phosphate buffer containing 150 mM NaCl, pH 7.2, and kept at 4 °C until use (at most 24 h after isolation). Prior to use, erythrocytes were collected by centrifugation, washed, resuspended in PBS (80 mM phosphate, 40 mM NaCl, and 10 mM KCl), pH 7.3, and then treated with DMPO and peroxynitrite at room temperature (25 ± 2 °C). Hemolysates were obtained by three freezing/thawing cycles, and the supernatant was collected by centrifugation. For some experiments, hemolysates were dialyzed twice against 0.1 M phosphate buffer, pH 7.4 (1:100 dilution factor each time).

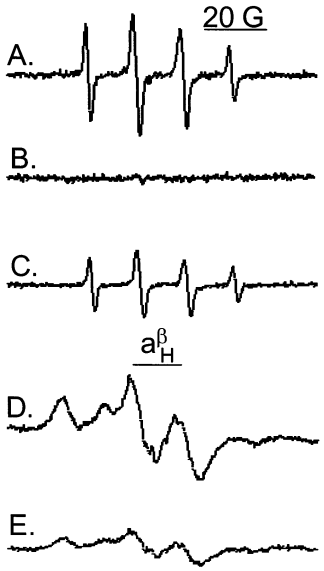

FIGURE 1: Representative EPR spectra of DMPO adducts obtained during the interaction of human erythrocytes with peroxynitrite. Except for (E), all the spectra were obtained 1 min after the addition of peroxynitrite to erythrocyte suspensions (20%, v/v) in PBS, pH 7.3, containing 50 mM DMPO. (A) Erythrocytes plus 1 mM peroxynitrite. (B) Erythrocytes plus 1 mM decomposed peroxynitrite. (C) Same as (A) with DMPO being added 2 min after peroxynitrite. (D) Erythrocytes plus 2.5 mM peroxynitrite. (E) Same as (D) after 7 min of incubation. Instrumental conditions: microwave power, 20 mW; time constant, 327.7 ms; scan rate, 0.3 G/s; gain, 3.99 $\times$ 10^5; modulation amplitude, 1 G, except for (D) and (E) where 5 G was used.

Non-protein Thiols. Erythrocytes were treated with peroxynitrite at room temperature and, after different incubation times, were lysed and deproteinized by dilution (1:10, v/v) with a solution of 2 M $HClO_4$ containing 4 mM DTPA. After centrifugation, the supernatants were neutralized with KOH and centrifuged again. Aliquots of the supernatants were diluted with phosphate buffer, pH 8.0, containing 0.25 mM DTNB and the nonprotein thiols determined by absorbance measurements at 412 nm (ϵ = 13.6 $\times$ 10^3 M^{-1} cm^{-1}) (*10*, *11*).

EPR Experiments. EPR spectra were recorded at room temperature (25 ± 2 °C) on a Bruker ER 200 D-SRC upgraded to an EMX instrument and equipped with a high-sensitivity cavity (4119HS). The incubation mixtures were transferred to a flat cell and the spectra recorded at room temperature at various incubation times.

RESULTS

Production of Glutathiyl and Hemoglobin-Derived Radicals. Addition of 1 mM peroxynitrite to an erythrocyte suspension (20% v/v) in PBS containing 50 mM DMPO led to the detection of an EPR spectrum whose parameters are characteristic of the DMPO/•SG (a_N = 15.2 G; a^{β}_H = 15.9 G) radical adduct (Figure 1A) (*4*). This signal was detectable with peroxynitrite concentrations from 0.1 to 2.0 mM and erythrocyte suspensions at concentrations higher than 5%. The DMPO/•SG radical adduct signal decayed with time but remained detectable up to 20 min of incubation. No EPR signal was detected in the absence of erythrocytes (data not shown) or upon the addition of previously decomposed peroxynitrite to erythrocytes (Figure 1B). The DMPO/•SG adduct was detectable even when DMPO was added to the

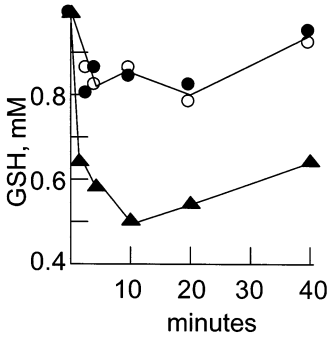

FIGURE 2: Time-dependent GSH depletion and recovery in erythrocyte suspensions (20%, v/v) treated with 1 mM peroxynitrite (▲), in untreated erythrocytes (○), and in erythrocytes treated with decomposed peroxynitrite (●). Incubation conditions and methods are as described in the Experimental Procedures. The values shown are the mean of three independent experiments.

erythrocyte suspension from 2 to 5 min after peroxynitrite addition (Figure 1C). Accordingly, kinetic measurements of nonprotein thiol (mostly GSH) depletion in erythrocyte suspensions treated with peroxynitrite showed that thiol levels keep decreasing up to 10 min after peroxynitrite addition and then start to be slowly recovered (Figure 2) as previously reported (*12*). These results indicate that glutathione oxidation and glutathiyl radical production occur through secondary reactions because more than 99% of the peroxynitrite entering the erythrocytes will decompose in a few milliseconds by reacting with intracellular oxyhemoglobin and carbon dioxide (*6*, *7*). When erythrocyte suspensions (20% v/v) were treated with higher peroxynitrite concentrations (≥2.5 mM), the EPR spectrum of the DMPO/•SG radical adduct was replaced by an immobile EPR spectrum (Figure 1D) that indicates trapping of a high molecular weight radical, certainly, a hemoglobin-derived radical (*3*). The DMPO/•hemoglobin radical adduct spectrum also decayed with time (Figure 1E; compare with Figure 1D).

The DMPO/•SG and DMPO/•hemoglobin radical adducts were also detected when the erythrocytes were lysed before being treated with peroxynitrite (Figure 3). However, as expected from the absence of a cellular membrane that minimizes extracellular peroxynitrite decay (*1*, *2*, *4*, *6*, *7*, *13*), lower concentrations of the oxidant were required to produce higher yields of radical adducts. For instance, an intense DMPO/•SG radical adduct signal was already detected with the addition of 0.1 mM peroxynitrite to hemolysates (Figure 3A). With 0.2−0.5 mM peroxynitrite, a composite EPR spectrum of the DMPO/•SG and DMPO/•-hemoglobin radical adducts was produced (Figure 3B), whereas 1 mM oxidant yielded mostly the DMPO/•hemoglobin radical adduct spectrum (Figure 3C). All spectra decayed with time but remained detectable up to 20 min of incubation time (for instance, compare parts C and D of Figure 3). Similar spectra were detected when DMPO was added to hemolysates from 2 to 5 min after peroxynitrite addition, although their intensities were lower and the contribution of the DMPO/•SG adduct became more pronounced (Figure 3E; compare with Figure 3C). These results suggest that the hemoglobin-derived radical is produced through secondary reactions as was the case for the glutathiyl radical (Figures 1C and 2).

The results described above were qualitatively the same in the presence of exogenously added carbon dioxide (1.5

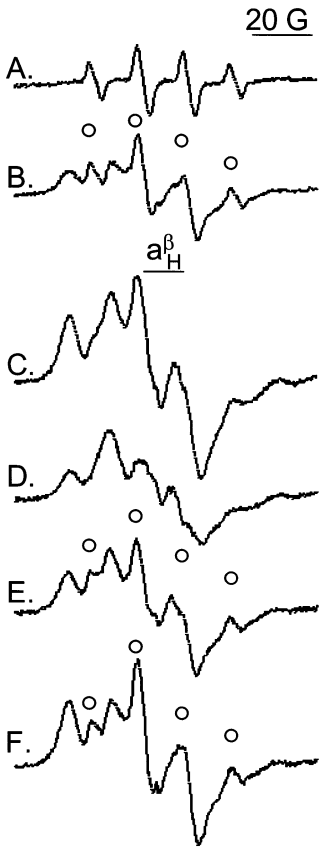

FIGURE 3: Representative EPR spectra of DMPO adducts obtained during the interaction of hemolysates with peroxynitrite. Except for (D), all the spectra were obtained 1 min after the addition of peroxynitrite to erythrocyte hemolysates (20%, v/v) in PBS, pH 7.3, containing 50 mM DMPO. (A) Hemolysates plus 0.1 mM peroxynitrite. (B) Hemolysates plus 0.5 mM peroxynitrite. (C) Hemolysates plus 1 mM peroxynitrite. (D) Same as (C) after 7 min of incubation. (E) Same as (C) with DMPO being added 2 min after peroxynitrite. (F) Same as (C) in the presence of 1.5 mM carbon dioxide. The positions of DMPO/thiyl radical adduct peaks are labeled with ○ in all spectra their contribution is apparent. Instrumental conditions: microwave power, 20 mW; time constant, 327.7 ms; scan rate, 0.3 G/s; modulation amplitude, 5 G; gain, 3.99 × 10^4.

mM). In erythrocytes, radical yields decreased for the same peroxynitrite concentration (data not shown). This was expected because the fast reaction between carbon dioxide and peroxynitrite will produce nitrogen dioxide and carbonate radical anion extracellularly (eq 3), reducing the concentration of oxidants that are able to enter erythrocytes (*1*, *2*, *4*, *6*, *7*, *13*). In the case of hemolysates, the spectra obtained always showed a greater contribution of the DMPO/•SG radical adduct (Figure 3E; compare with Figure 3C) as expected from the oxidation of glutathione by the radicals produced from the reaction of peroxynitrite with carbon dioxide (*2*, *4*, *10*).

Characterization of the Hemoglobin-Derived Radicals. The DMPO/•hemoglobin radical adduct detected under our experimental conditions (Figures 1D,E and 3C,D) could be hemoglobin-tyrosyl radical previously reported to be produced upon peroxynitrite addition to erythrocytes (*3*). We confirmed these previous studies, and indeed, a hemoglobin-tyrosyl radical ($g = 2.0048$, peak to through width = 23 G) (14) was detected by direct EPR upon the addition of 1 mM peroxynitrite to both erythrocytes and hemolysates (data not shown). In the presence of DMPO, however, the immobilized

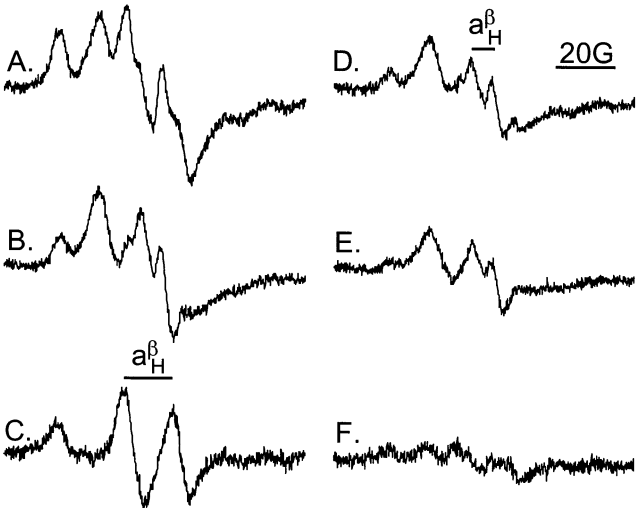

FIGURE 4: Effects of *N*-ethylmaleimide upon the EPR spectra obtained during the interaction of dialyzed hemolysates with peroxynitrite. The spectra were obtained 1 (left panel) and 7 (right panel) min after the addition of peroxynitrite (1 mM) to dialyzed hemolysates (4 mM heme-hemoglobin) in PBS, pH 7.3, containing 50 mM DMPO. (A) Dialyzed hemolysates. (B) Dialyzed hemolysates pretreated with 8 mM N-ethylmaleimide for 30 min. (C) Computer subtraction of (A) − (B). (D) Same as (A) after 7 min of incubation. (E) Same as (B) after 7 min of incubation. (F) Computer subtraction of (D) − (E). Instrumental conditions: microwave power, 20 mW; time constant, 327.7 ms; scan rate, 0.3 G/s; gain, 3.99×10^4; modulation amplitude, 2 G.

spectrum obtained in erythrocytes (Figure 1D,E) was quite different from the one obtained in hemolysates (Figure 3C,D). In addition, both of these spectra presented a β hydrogen splitting constant value of around 14 G, which was considerably higher than those reported for other DMPO/•tyrosyl-protein radical adducts (*15*−*17*) and more consistent with DMPO/•thiyl radical adducts such as the DMPO/•SG itself (Figure 3, marked peaks) or a DMPO/•cysteinyl-protein radical adduct (*4*, *17*−*21*).

Consequently, to better characterize the immobilized radical adduct, hemolysates were dialyzed to remove glutathione and treated or not with the thiol-blocking reagent *N*-ethylmaleimide (2 times excess over heme-hemoglobin) for 30 min before the addition of DMPO and peroxynitrite (Figure 4). Pretreatment of oxyhemoglobin with *N*-ethylmaleimide (Figure 4B) inhibited the overall intensity of the 1 min EPR signal (Figure 4A) by about 30% as calculated by double integration of both spectra. This value should correspond to the yield of the DMPO/•cysteinyl-hemoglobin radical adduct obtained in dialyzed hemolysates. Its EPR spectrum, obtained by computer subtraction of thiol-blocked hemoglobin (Figure 4B) from the native hemoglobin (Figure 4A) spectrum, presented a β hydrogen splitting constant of 15.4 G (Figure 4C), which is consistent with those previously reported for other DMPO/•cysteinyl-protein radical adducts (*17*−*21*). The DMPO/•cysteinyl-hemoglobin radical adduct rapidly decayed in dialyzed hemolysates because its contribution to the spectra scanned 7 min after peroxynitrite addition was barely detectable (Figure 4D; compare with Figure 4A). Actually, at longer incubation times, thiol-free (Figure 4D) and thiol-blocked hemoglobin (Figure 4E) yielded the same EPR spectrum. Its β hydrogen splitting constant presented a value of 8.8 G, which is consistent with those previously reported for DMPO/•tyrosyl-protein radical adducts (*15*−*17*). Thus, the EPR spectrum of both the DMPO/•tyrosyl- (Figure 4D,E) and DMPO/•cysteinyl-hemoglobin (Figure 4C) radical adducts of human hemoglobin was characterized. These adducts were always detectable when dialyzed hemolysates were treated with peroxynitrite, but their relative yields changed with storage. With up to one week of storage at 4 °C, the main detectable adduct was the DMPO/•tyrosyl-hemoglobin radical adduct as shown in Figure 4. After one month, the hemoglobin-tyrosyl radical remained detectable by direct EPR, but the main radical detected by spin trapping was the DMPO/cysteinyl-hemoglobin radical adduct (data not shown). These results indicate that changes in hemoglobin structure may facilitate electron transfer from the hemoglobin-tyrosyl radical to a hemoglobin-cysteine residue (*19*, *22*−*24*). The occurrence of electron transfer from the hemoglobin-tyrosyl radical to a cysteine residue of another hemoglobin monomer is supported by the fact that oxyhemoglobin concentration increased the relative yield of the DMPO/•cysteinyl-hemoglobin radical adduct, which was higher in erythrocytes (Figure 1D,E) than in their corresponding dialyzed hemolysates (Figure 4) (see the Discussion).

It should be mentioned that both radical adducts, the DMPO/•tyrosyl-hemoglobin and DMPO/•cysteinyl-hemoglobin, presented an EPR spectrum characteristic of highly immobilized nitroxides in contrast with those previously reported for other DMPO/•protein radical adducts (*15*−*17*, *21*) with the exception of the DMPO/•cysteinyl-albumin (*19*, *20*) and the DMPO/•cysteinyl radical adducts from rat hemoglobin (*18*). The spectrum of the latter, however, is markedly different from the spectrum characterized here for human hemoglobin (Figure 4C). These highly immobilized spectra may reflect highly constrained radical adducts located in hydrophobic cores. Alternatively, they may reflect the addition of the EPR spectra of similar but diverse radical adducts due to the tetrameric hemoglobin structure. Accordingly, mass spectrometry analysis of oxyhemoglobin modified by peroxynitrite demonstrated oxidation of diverse tyrosine (α42, β130, α24) residues (*25*).

DISCUSSION

Our results showed that peroxynitrite addition to erythrocytes led to the oxidation of both intracellular hemoglobin and glutathione to produce the corresponding hemoglobin-tyrosyl, hemoglobin-cysteinyl, and glutathiyl radicals that were trapped by DMPO even when the spin trap was added after peroxynitrite decomposition (Figure 1C). To characterize all of the detected radicals, it was necessary to compare the results obtained with eryhrocytes, hemolysates, and dialyzed hemolysates (Figures 1−4). Taken together, the results indicate that glutathiyl, hemoglobin-cysteinyl, and hemoglobin-tyrosyl radicals are produced in erythrocytes from secondary reactions because although protein-tyrosyl radicals can be long-lived (*3*), thiyl radicals are unstable and react fast with oxygen among other targets (*10*, *11*). Accordingly, the main peroxynitrite target in erythrocytes is oxyhemoglobin, which is oxidized to methemoglobin (*6*, *7*). In cell-free systems, this reaction has been previously shown to proceed through intermediate formation of ferryl-hemoglobin and to follow stoichiometries varying from 2:1 to 1:2 (protein heme:oxidant) depending on the pH and molar reactant ratios (*3*, *6*, *7*, *25*−*28*). Most likely the reaction starts

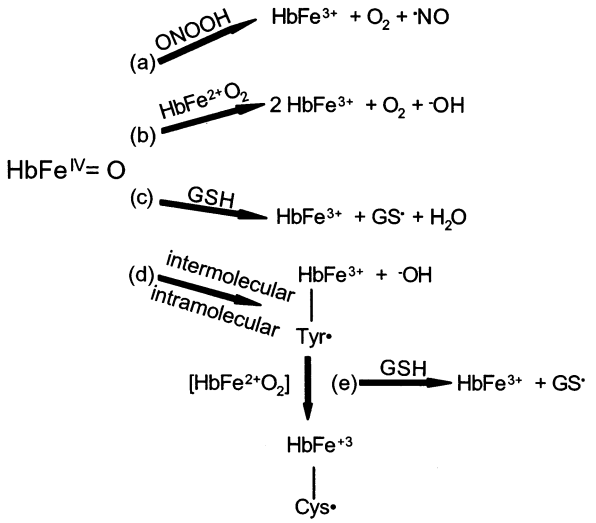

FIGURE 5: Schematic representation of ferryl-hemoglobin decay pathways in erythrocytes. The scheme is based on the results reported here and previously published data (*3*, *6*, *7*, *25*−*29*).

with a direct two-electron oxidation to produce an analogue of compound II of peroxidase enzymes (eq 4). This is an oxidizing intermediate that may decay by several routes depending on the protein:peroxynitrite ratio and the environment (Figure 5) (*3*, *6*, *7*, *25*−*28*).

$$HbFe^{2+}O_2 + ONOOH \rightarrow HbFe^{IV}{=}O + NO_2^- + O_2 + H^+ \quad (4)$$

Consequently, in erythrocytes, oxidation of oxyhemoglobin by the addition of peroxynitrite produces ferryl-hemoglobin, which, in turn, oxidizes its own amino acid residues to produce hemoglobin-tyrosyl and hemoglobin-cysteinyl radicals and also oxidizes intracellular glutathione to produce the glutathiyl radical (Figure 5). Most likely, the hemoglobin-tyrosyl radical is produced by intramolecular oxidation of tyrosine residues in the vicinity of the ferryl intermediate (*3*, *15*, *16*, *28*) (Figure 5, route d). The same route is likely to be responsible for the production of the hemoglobin-cysteinyl radical through inter- and/or intramolecular electron transfer from the initially produced hemoglobin-tyrosyl radical to a hemoglobin-cysteine residue. Indeed, electron transfer from one residue to another in the same and in other molecules is a common process in proteins (*19*, *22*−*24*). The direct oxidation of intracellular glutathione by ferryl-hemoglobin (Figure 5, route c) can be proposed because glutathione oxidation by the analogous ferryl-myoglobin has been shown to be rapid ($k = 1 \times 10^4$ M^{-1} s^{-1}) and to produce the glutathiyl radical (*29*). In addition, the possibility of glutathione reacting with the hemoglobin-derived radicals in a process that would repair them cannot be excluded (Figure 5, route e) (*29*). Such a route would explain why the DMPO/•SG radical was detectable with peroxynitrite concentrations lower than those required to detect the DMPO/•hemoglobin radical adducts (Figures 1 and 3). Since the spin trapping technique was used to detect the radicals produced in peroxynitrite-treated erythrocytes, however, there is an alternative explanation for the detection of the DMPO/•SG radical adduct with peroxynitrite concentrations lower than those required for detecting the DMPO/•hemoglobin radical adducts, i.e., a higher accessibility of the low molecular weight glutathiyl radical to DMPO as compared with that of the high molecular weight hemoglobin-derived radicals. Indeed, the detection of spin-trapped radical adducts depends on their stability and also on the reaction rate of the spin-trapping reaction (*5*, *30*). For instance, protein-tyrosyl radicals that are usually stable enough to be detected by direct EPR (*3*, *15*, *16*) are less reactive toward DMPO than protein-thiyl radicals (*17*). In agreement, the addition of 1 mM peroxynitrite to erythrocytes produced the hemoglobin-tyrosyl radical in concentrations that were not high enough to be detectable by EPR spin trapping (Figure 1) but were sufficient to be detectable by direct EPR (see the Results).

The production of the hemoglobin-tyrosyl radical (Figure, 5 route d) through an intramolecular electron-transfer process is supported by several lines of evidence (*3*, *14*−*16*, *28*). The production of the hemoglobin-cysteinyl radical, however, is likely to occur by both intra- and intermolecular electron transfer because both hemoglobin chains are oxidized to ferryl-hemoglobin but only the β chain has a cysteine residue (β93) that is accessible to oxidation (*18*, *25*). In addition, the relative yield of DMPO/•cysteinyl-hemoglobin in comparison with that of the DMPO/•tyrosyl-hemoglobin radical adduct was higher in erythrocytes (Figure 1D,E), which possess higher oxyhemoglobin levels (intracellular concentration), than in hemolysates (Figures 3C,D and 4). This is consistent with an intermolecular electron-transfer process but does not prove it. Indeed, the factors that control electron-transfer processes in proteins have yet to be discovered (*19*, *22*−*24*). Likewise, the reaction of spin traps with protein-derived radicals remains to be fully understood. As described above (Results), aged dialyzed hemolysates produced higher relative yields of the DMPO/•cysteinyl-hemoglobin radical adduct in comparison with fresh hemolysates (Figure 4). Whether structural alterations of hemoglobin in aged hemolysates facilitate electron transfer from the hemoglobin-tyrosyl radical to a cysteine residue and/or alter the ability of DMPO in trapping hemoglobin-derived radicals remains to be established.

As pointed out above, the spin-trapping technique has limitations because the detected radical adducts and their concentrations do not necessarily reflect the main produced radicals or their relative importance in a given process (*5*, *30*). Consequently, at this point, it is impossible to establish all the mechanistic details of the interaction between peroxynitrite and erythrocytes (*3*, *6*, *7*, *25*). Relevantly, however, the production of glutathiyl, hemoglobin-cysteinyl, and hemoglobin-tyrosyl radicals was unequivocally proved with the use of the spin trap DMPO, and the reactions summarized in Figure 5 account for most of the results described here for up to 30 min incubations (Figures 1−4). At longer incubation times, other processes are likely to become relevant because of the reactivity of the initially produced species (eq 4 and Figure 5). For instance, nitrite oxidizes hemoglobin in a reaction that produces nitrogen dioxide that can further oxidize both hemoglobin (*31*−*33*) and glutathione (*10*, *11*). The reaction of the glutathiyl radical with glutathione produces the corresponding disulfide radical anion that reacts with oxygen to produce the superoxide anion radical and, hence, hydrogen peroxide (*10*, *11*) that can further oxidize hemoglobin (*14*, *29*, *31*−*33*). The secondary reactions of the glutathiyl radical may be partially responsible for the fact that the DMPO/•cysteinyl-hemoglobin radical

adduct remained detectable for longer times in erythrocytes (Figure 1D,E) and hemolysates (Figure 3C,D) than in dialyzed hemolysates (Figure 4A,D). Overall, the relevance of all these reactions will be dependent on the concentrations of the initially produced nitrite and glutathiyl radical and, hence, the peroxynitrite concentrations that enter erythrocytes (eq 4 and Figure 5).

In conclusion, our results confirm and extend previous studies demonstrating that oxyhemoglobin is the main target of peroxynitrite in erythrocytes (*3*, *6*, *7*). As we first demonstrated here, the produced ferryl-hemoglobin oxidizes its own amino acids and, most probably, amino acids from other hemoglobin monomers to produce hemoglobin-tyrosyl and hemoglobin-cysteinyl radicals. The EPR spectrum of both DMPO/•cysteinyl-hemoglobin (a^{β}_{H} = 15.4 G) and DMPO/•tyrosyl-hemoglobin (a^{β}_{H} = 8.8 G) radical adducts was characterized. The produced ferryl-hemoglobin also oxidizes intracellular glutathione to produce the glutathiyl radical. This species may also be produced by the reaction of glutathione with hemoglobin-derived radicals. At low peroxynitrite concentrations that are more relevant for in vivo situations, oxidation of glutathione by the hemoglobin-derived radicals may predominate (Figure 5, route e). This would provide a route for repair because both methemoglobin and the glutathiyl radical, via oxidized glutahione (GSSG), can be reduced back by erythrocyte enzymatic systems. Thus, erythrocytes may be efficient peroxynitrite scavengers in vivo through the coupled action of oxyhemoglobin and glutathione.

In a broader scenario, our results further indicate that intracellular oxidation of glutathione to the glutathiyl radical is likely to be an important consequence of peroxynitrite production by most cells (*2*, *4*). The glutathiyl radical may result from the oxidation of glutathione by the radicals that are produced in the reaction of peroxynitrite with the ubiquitous carbon dioxide, that is, nitrogen dioxide and carbonate radical anion (eq 3) (*2*, *4*). Alternatively, as shown here, the glutathiyl radical may be produced from glutathione oxidation by ferryl species generated during the interaction of peroxynitrite with hemoproteins that are equally ubiquitous in cells.

REFERENCES

1. Radi, R., Denicola, A., Alvarez, B., Ferrer-Sueta, G., and Rubbo, H. (2000) in *Nitric oxide: Biology and Pathobiology* (Ignarro, L. J., Ed.) pp 57−89, Academic Press, New York.
2. Augusto, O., Bonini, M. G., Amanso, A. M., Linares, E., Santos, C. C. X., and De Menezes, S. L. (2002) *Free Radical Biol. Med. 32*, 849−859.
3. Minetti, M., Scorza, G., and Pietraforte, D. (1999) *Biochemistry 38*, 2078−2087.
4. Menezes, S. L, and Augusto, O. (2001) *J. Biol. Chem. 276*, 39879−39884.
5. Mottley, C., and Mason, R. P. (1989) in *Biological Magnetic Resonance* (Berliner, L. J., and Reuben, J., Eds.) Vol. 8, pp 489−545, Plenum Publishing, New York.
6. Denicola, A., Souza, J. M., and Radi, R. (1998) *Proc. Natl. Acad. Sci. U.S.A. 95*, 3566−3571.
7. Romero, N., Denicola, A., Souza, J. M., and Radi, R. (1999) *Arch. Biochem. Biophys. 368*, 23−30.
8. Schafer, F. Q., and Buettner, G. R. (2001) *Free Radical Biol. Med. 30*, 1191−1212.
9. Kissner, R., Nauser, T., Bugnon, P., Lye, P. G., and Koppenol, W. H. (1997) *Chem. Res. Toxicol. 10*, 1285−1292.
10. Bonini, M. G., and Augusto, O. (2001) *J. Biol. Chem.* 276, 9749−9754.
11. Quijano, C., Alvarez, B., Gatti, R. M., Augusto, O., and Radi, R. (1997) *Biochem. J. 322*, 167−173.
12. Soszynski, M., and Bartosz, G. (1996) *Biochim. Biophys. Acta 1291*, 107−114.
13. Khairutdinov, R. F., Coddington, J. W., and Hurst, J. K. (2000) *Biochemistry 39*, 14238−14249.
14. Giulivi, C., and Cadenas, E. (1998) *Free Radical Biol. Med. 24*, 269−279.
15. Gunther, M. R., Tschirret-Guth, R. A., Witkowska, H. E, Fann, Y. C., Barr, D. P., Ortiz de Montellano, P. R., and Mason, M. P. (1998) *Biochem. J. 330*, 1293−1299.
16. Gunther, M. R., Sturgeon, B. E., and Mason, R. P. (2000) *Free Radical Biol. Med. 28*, 709-719.
17. Witting, P. K., Douglas, D. J., and Mauk, A. G. (2000) *J. Biol. Chem. 275*, 20391−20398.
18. Maples, K. R., Eyer, P., and Mason, R. P. (1990) *Mol. Pharmacol. 37*, 311−318.
19. Davies, M. J., Gilbert, B. C., and Haywood, R. M. (1993) *Free Radical Res. Commun. 18*, 353−367.
20. Gatti, R. M., Radi, R., and Augusto, O. (1994) *FEBS Lett. 348*, 287−290.
21. Chen, Y-R., Gunther, M. R., and Mason, R. P. (1999) *J. Biol. Chem. 274*, 3308−3314.
22. Silvester, J. A., Timmins, G. S., and Davies, M. J. (1998) *Free Radical Biol. Med. 24*, 754−766.
23. Deterding, L. J., Barr, D. P., Mason, R. P., and Tomer, K. B. (1998) *J. Biol. Chem. 273*, 12863−12869.
24. Ostdal, H., Andersen, H. J., and Davies, M. J. (1999) *Arch. Biochem. Biophys. 362*, 105−112.
25. Minetti, M., Pietraforte, D., Carbone, V. Salzano, A. M., Scorza, G., and Marino, G. (2000) *Biochemistry 39*, 6689−6697.
26. Alayash, A. I., Ryan, B. A. B., and Cashon, R. E. (1998) *Arch. Biochem. Biophys. 349*, 65−73.
27. Exner, M. E., and Herold, S. (2000) *Chem. Res. Toxicol. 13*, 287−293.
28. Bourassa, J. L., Ives, E. P., Marqueling, A. L., Shimanovich, R., and Groves, J. T. (2001) *J. Am. Chem. Soc. 123*, 5142−5143.
29. Romero, F. J., Ordoñez, I., Arduini, A., and Cadenas, E. (1992) *J. Biol. Chem. 267*, 1680−1688.
30. Augusto, O. (1989) In *Handbook of Biomedicine of Free Radicals and Antioxidants* (Miquel, J., Ed.) Vol. 3, pp 193−208, CRC Press, Boca Raton, FL.
31. Kosaka, H., Imaizumi, K., and Tyuma, I. (1981) *Biochim. Bipohys. Acta 702*, 237−241.
32. Winterbourn, C. (1985) *Environ. Health Perspect. 64*, 321−330.
33. Lissi, E. (1998) *Free Radical Biol. Med. 24*, 1536−1536.

BI0262202